New reaction classes in the kinetic modeling of low temperature oxidation of n-alkanes

Eliseo Ranzi *, Carlo Cavallotti, Alberto Cuoci, Alessio Frassoldati, Matteo Pelucchi, Tiziano Faravelli

Department of Chemistry, Materials, and Chemical Engineering, Politecnico di Milano, Piazza Leonardo da Vinci 32, 20133 Milano, Italy

Received 21 July 2014
Received in revised form 24 November 2014
Accepted 24 November 2014
Available online 16 December 2014

1. Introduction

The understanding of the elementary reactions that govern the chemistry of low-temperature combustion and autoignition in internal combustion engines is in continuous progress, mainly due to the rapid advances both in theoretical kinetics and in experimental methods [1]. After several comprehensive reviews [2–6], the more recent work of Zádor et al. [1] highlighted the fundamental role of key elementary reactions involved in the low-temperature oxidation and ignition chemistry, where reactions of peroxy and hydroperoxy radical species are important [7]. In particular, they emphasized the ways in which computational chemistry and improved experimental capabilities enable a more detailed characterization of complex oxidation reactions. They also concluded that while the reactions of alkyl radicals with O_2 are better clarified, the mechanism of the second oxygen addition and related chemistry is nowadays an important unanswered question for ignition chemistry research [7]. Moreover, new experimental data of low-temperature oxidation of propane, n-butane and n-heptane in a jet stirred reactor (JSR) were recently presented and discussed [8–14]. The joint research efforts of Nancy and Hefei produced very detailed experimental measurements of reaction products of stoichiometric mixtures at low temperatures and atmospheric pressure in a JSR. The reaction products were analyzed using gas chromatography analysis and mass spectrometry. The mass spectrometer was combined with tunable synchrotron vacuum ultraviolet photoionization and coupled with a JSR via a molecular-beam sampling system. In this way, a large detail of reaction products of propane and n-butane oxidation have been quantified, including hydrogen peroxide and several oxygenated organic compounds, such as ketones, cyclic ethers, alcohols, acetic acid, alkyl- and carbonyl-hydroperoxides [9]. Similar attention was also paid to the formation of reaction products involved in the low-temperature oxidation of n-heptane highlighting that diones and di-oxygenated products other than carbonyl-hydroperoxides (CHP) or keto-hydroperoxides are important intermediates in the low-temperature oxidation of n-alkanes, but their formation was usually not accounted for in the detailed or lumped kinetic models of hydrocarbon fuel combustion [15–22].

* Corresponding author. Fax: +39 02 2399 3280.
E-mail address: eliseo.ranzi@polimi.it (E. Ranzi).

The aim of this paper is to critically revise the low temperature oxidation mechanism, taking advantage of this new comprehensive and detailed information. Moving from the systematic deviations between model predictions and experimental measurements, Section 2 discusses the new reaction classes added to the low temperature oxidation mechanism of hydrocarbon fuels. Particularly, H-abstraction reactions on hydroperoxides and carbonyl-hydroperoxides are firstly analyzed. Then, successive molecular reactions of carbonyl-hydroperoxides, as well as recombination/disproportionation reactions of peroxy radicals are also discussed. Section 3 presents some theoretical calculations to determine preliminary rate constants for relevant reactions used in this work. Section 4 finally presents complete comparisons between model predictions and experimental data of the low temperature oxidation of propane and n-butane.

2. Low temperature oxidation mechanism and new reaction classes

Since the pioneering work of Westbrook et al. [23], who proposed the first detailed low- and high-temperature oxidation mechanism of n-heptane, the chain radical oxidation mechanism of n-alkanes, with the formation of extremely reactive hydroperoxide species, was identified and commonly accepted [18,24,25]. Figure 1 schematically shows the oxidation mechanism of propane [26]. The two addition reactions of molecular oxygen to alkyl radicals ($R^{\cdot}$ and $^{\cdot}QOOH$), together with the successive isomerization reactions of peroxy radicals ($ROO^{\cdot}$ and $^{\cdot}OOQOOH$), and the formation of hydroperoxide and carbonyl-hydroperoxide species are critical to the low temperature oxidation chemistry of hydrocarbon fuels [7].

As clearly discussed by Battin-Leclerc [6], the formation of peroxides is extremely important, because they include an O–OH bond, which can easily be broken and lead to the formation of two radicals, which can in their turn react with fuel molecules to give alkyl radicals. These degenerate branching steps involve an increase of the number of radicals, which induces an exponential acceleration of reaction rates leading in some conditions to spontaneous autoignition. The works of Curran et al. [18,27] defined the oxidation mechanisms for primary reference fuels in terms of 25 specific reaction classes and exploited a modular form for the construction of kinetic schemes that is largely accepted and employed. Due to the low dissociation energy of the O–OH bond and the high reactivity of hydroperoxide species, only the class of unimolecular decomposition reactions was considered for these species. This oxidation mechanism was extensively applied to different linear and branched alkanes, up to normal hexadecane [28–30], as well as heavy branched alkanes [22,31].

The recent data obtained by Nancy and Hefei research teams [8–14] allow to critically revise and highlight the limits of the existing low temperature mechanisms in the proper prediction of oxygenated species. As already observed by Herbinet et al. [9,10] in n-butane and n-heptane oxidation, while detailed kinetic models [8] satisfactorily reproduce the global reactivity and the usual oxidation products, their predictions partially deteriorate in the case of the formation of organic acids and species with two carbonyl groups. To account for these discrepancies, Battin-Leclerc et al. [8,32] and Herbinet et al. [10] already analyzed possible pathways for the formation of acids and molecules including two carbonyl groups, or molecules with one carbonyl and one alcohol. Despite the addition of these new reaction pathways, the formation of carboxylic acids and compounds with two carbonyl groups was not completely explained, and they observed the need of an increased accuracy of the kinetic models [33].

The presence of very sharp peaks of some oxygenated species at low temperatures [10] can be well explained on the basis of successive reactions of carbonyl-hydroperoxides involving activation energies lower than those typical of the unimolecular decomposition reactions, i.e. the O–OH bond dissociation energy (40–45 kcal/mol). Indeed, the formation of molecules including two carbonyl groups can be easily explained on the basis of H-abstraction reac-

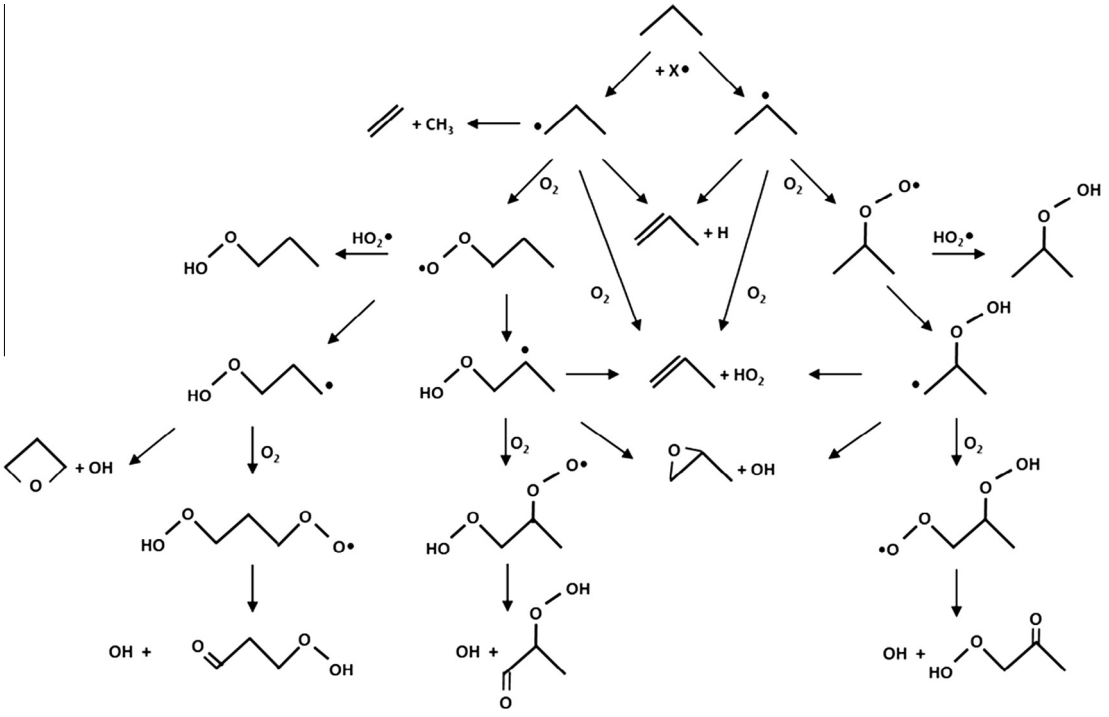

Fig. 1. Chain radical mechanism of propane oxidation.

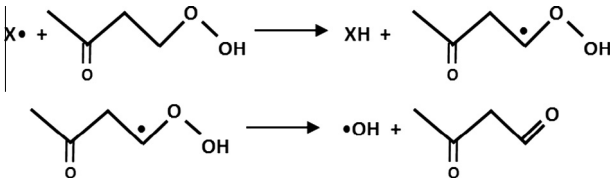

Fig. 2. H-abstraction from 2-acetyl-ethyl hydroperoxide and radical decomposition to form 3-oxobutanal.

tions on the site of the hydroperoxyl substitution and the subsequent decomposition of the O–OH bond, as shown in Fig. 2. Thus, 3-oxobutanal can be obtained from H-abstraction on 2-acetyl-ethyl hydroperoxide.

As it will be better shown in Section 3, the intermediate C_4 radical is instantaneously decomposed to form OH radical and the corresponding 3-oxobutanal. At temperatures lower than 600 K and the oxidation conditions here analyzed, OH radicals largely dominate the H-abstraction reactions and this radical reaction to form C_4-molecules including two carbonyl groups can also prevail over the previously proposed reaction channels [8,10,32]. At these low temperatures, the H-abstraction reactions on carbonyl-hydroperoxides can play a significant role, thus decreasing the chain branching effect of the competing initiation reactions. The net consequence is a reduction of the overall conversion, at temperatures lower than 550–600 K, while only at higher temperatures the unimolecular decomposition of CHP remains the dominant reaction path. Referring to the low temperature oxidation of n-butane [12], Fig. 3 shows the clear reduction of reactivity and the better agreement with the experiments mainly at 550–600 K. Moreover, the sharp peak at the very low temperatures (~600 K) in the production of C_4-molecules including two carbonyl groups, previously completely disregarded, is reasonably reproduced.

Similar considerations on the importance of the H-abstraction reactions need to be extended also to all the hydroperoxides. Thus, butanal and methyl-ethyl-ketone (MEK) are the expected products of H-abstractions on C_4-hydroperoxides.

All these considerations clearly confirm the importance of successive reactions of hydroperoxide species. With reference to the low temperature oxidation mechanism of propane, Figs. 4 and 5 show the H-abstraction reactions on C_3-hydroperoxides and the most favored C_3-carbonyl-hydroperoxides, respectively.

In their general form, the following classes of H-abstraction reactions are likely to be included in the low temperature oxidation mechanism of hydrocarbon fuels:

(a) H-abstractions on alkyl-hydroperoxides:

$$X^{\cdot} + C_nH_{2n+1}OOH \rightarrow XH + {}^{\cdot}C_nH_{2n}OOH \rightarrow XH + C_nH_{2n}O + {}^{\cdot}OH$$

(b) H-abstractions on carbonyl-hydroperoxides:

$$X^{\cdot} + OC_nH_{2n-1}OOH \rightarrow XH + OC_nH_{2n-2}O + {}^{\cdot}OH$$

$$X^{\cdot} + OC_nH_{2n-1}OOH \rightarrow XH + C_mH_{2m-2}O + C_kH_{2k}O + {}^{\cdot}OH \quad (m+k=n)$$

$$X^{\cdot} + OC_nH_{2n-1}OOH \rightarrow XH + C_nH_{2n-2}O + {}^{\cdot}HO_2$$

These H-abstraction reactions on hydroperoxides and carbonyl-hydroperoxides, whose kinetic parameters are reasonably estimated on the basis of analogy and similarity rules [34] have already been applied to atmospheric chemistry studies [35–37]. For the first time, they are included in the kinetic model of hydrocarbon fuel combustion, to justify the formation of some oxygenated species. The role of these H-abstraction reactions, as well as the importance of molecular reactions involving carbonyl-hydroperoxides is better highlighted through the systematic comparisons between model predictions and experimental data reported in Section 4.

As far as the formation of organic acids is concerned, recently Jalan et al. [38] presented new reaction pathways of ketohydroperoxides relevant to low-temperature gas phase oxidation of propane. Ab initio calculations identified new exothermic reactions forming a cyclic peroxide isomer, which decomposes via concerted reactions into carbonyl and carboxylic acid products (Korcek mechanism). This reaction is very useful to explain the formation of formic and acetic acids, mainly at low temperatures and in liquid phase. The same reaction path allows also to explain the formation of propanoic acid from CHPs of C_4 and heavier species.

Moreover, an important source of acetic acid is the recombination/disproportionation reaction of peracetyl ($CH_3COOO^{\cdot}$) and methyl-peroxy radicals ($CH_3O_2^{\cdot}$):

$$CH_3COOO^{\cdot} + CH_3O_2^{\cdot} \rightarrow CH_3COOH + CH_2O + O_2$$

This reaction was already considered in a previous paper on methane oxidation, where the acetaldehyde low temperature reactions were also discussed [39]. Similarly, the recombination/disproportionation of alkyl-peroxy radicals forms O_2 and a di-alkyl-peroxide, which rapidly forms an alcohol and a carbonyl component. Thus, propyl peroxide radicals can form propanol and propanal:

$$C_3H_7OO^{\cdot} + C_3H_7OO^{\cdot} \rightarrow O_2 + C_3H_7OOC_3H_7$$

$$C_3H_7OOC_3H_7 \rightarrow C_3H_7OH + C_2H_5CHO$$

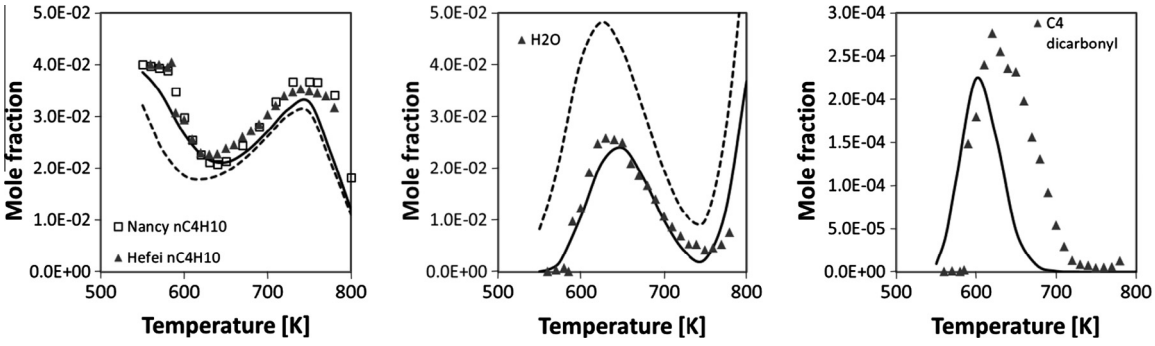

Fig. 3. Oxidation of n-butane in jet stirred reactor (n-butane/O_2/Ar = 4/26/70 mol%; 1.04 atm; residence time 6 s) [9,12]. Comparison of experimental mole fractions of n-butane, water, and C_4-molecules including two carbonyl groups measured at Nancy [squares] and Hefei [triangles] with model predictions with [solid lines] and without the new reactions [dashed lines].

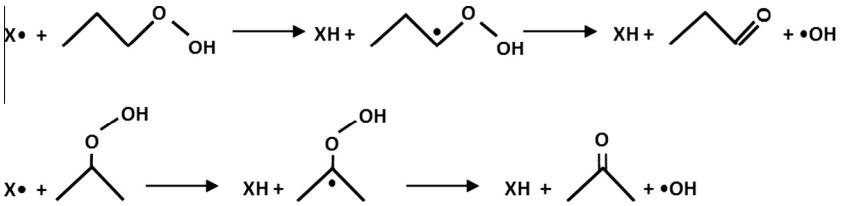

Fig. 4. H-abstraction reactions on propyl-hydroperoxides to form propanal and acetone.

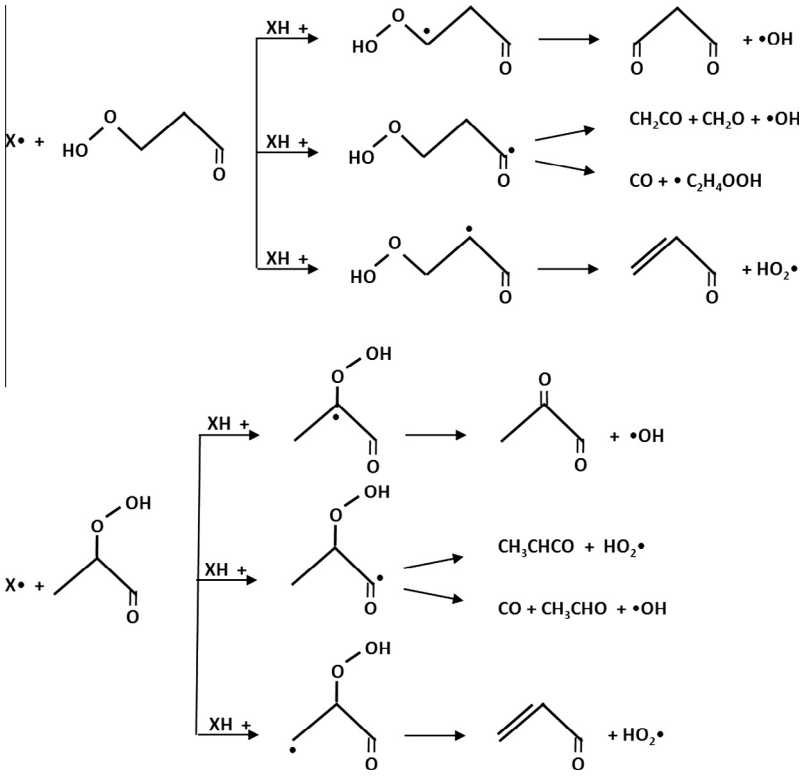

Fig. 5. H-abstraction reactions on the most favored C3-carbonyl-hydroperoxides.

Kinetic parameters for this reaction class are similar to those for the recombination reactions (Classes 15 and 16), as suggested by Curran et al. [18,27].

Thus, in addition to the 25 reaction classes usually considered in the low and high temperature oxidation schemes of alkanes [18,27], the following new reaction classes are here included:

1. H-abstraction reactions on alkyl and carbonyl-hydroperoxides.
2. Molecular reactions of carbonyl-hydroperoxides to form organic acids (Korcek mechanism).
3. Recombination/disproportionation reactions of peroxy radicals.

The approach used to validate the capability of the proposed reaction mechanism is based on the comparison with experimental measurements for propane and n-butane and on the use of theoretical calculations to determine preliminary rate constants for reaction channels for which no estimate based on analogy rules is possible. This was useful both to check the predictive capability of the similarity and analogy rules for some key reactions, as well as to provide preliminary estimates of rate constants of molecular processes that can be hardly determined through analogy. The purpose of these calculations, and more in general of the present work, is not to provide the most accurate estimate of the rate constant of the investigated reactions, but rather to identify a set of reactions that have the potential to contribute significantly to the low temperature reactivity of the investigated systems. For this purpose the theoretical rate constant estimate was performed at a level that allowed to evaluate rate parameters with an uncertainty factor of about three, which, combined with the satisfactory comparisons with experimental data, is useful to determine whether a reaction channel has the potential to have a significant impact on the system reactivity or not. All the rate constants here determined were eval-uated using conventional transition state theory calculating the necessary parameters either using the CBS-QB3 method or at the CCSD(T) level with extension to the complete basis set (CBS) using geometries and vibrational frequencies calculated at the M062X/6-311+G(d,p) level. The rate constant was corrected for tunneling using the Eckart model. The CBS extrapolation was performed through a scheme developed by Martin [40] using single point ener-gies computed with the aug-cc-pVDZ and aug-cc-pVTZ basis sets [41]. One reaction that has multireference character was investi-gated through CASPT2 calculations. All calculations were per-formed using the G09 suite of programs [42], except for the CCSD(T) and CASPT2 calculations, which were performed using Molpro 2008.1 [43].

3. Theoretical rate constant calculations and estimation

The theoretical analysis was focused on three different sets of reactions:

3.1. H-abstractions from the hydroperoxyl substitution site.
3.2. Carbonyl-hydroperoxide decomposition through the Korcek mechanism.
3.3. Molecular decomposition of acetyl-methyl-hydroperoxide.

The calculated unimolecular rate constants are high-pressure values, though at atmospheric pressure and between 500 and 700 K, where these reactions are most likely to play a significant role, the pressure dependence is expected to be small.

3.1. H-abstractions from the hydroperoxyl substitution site

The reactions of H-abstraction from carbonyl-hydroperoxides play an important role, as they are the main source of dicarbonyl compounds, as shown in Fig. 2. It was thus decided to determine the rate constant for one of these reaction channels, namely H-abstraction of the hydrogen atoms from a primary carbon atom functionalized with the hydroperoxyl group, as this is the one for which analogy rules are least established. The molecular model used in the simulations was 2-acetyl-ethyl-hydroperoxide ($CH_3COCH_2CH_2OOH$), whose reactivity is expected to be the same as that of 2-formyl-ethyl-hydroperoxide (C_3CHP). The considered extracting agent is the OH radical, as it is the most effective radical in the conditions considered in the present study. Simulations were performed for the two minimum energy conformers of $CH_3COCH_2CH_2OOH$. Abstraction is possible from two H atoms, which are differentiated by the relative orientation of the OH group of the OOH moiety. Two distinct rate constants were thus computed for each conformer, which were distinguished as cis or trans depending on the proximity to the OOH group. The rate constants were then summed up after performing a Boltzmann weight of the relative population of the two conformers and a global rate constant was determined. Further computational details are reported in the Supplemental Material.

The rate constants of the four reactions calculated using CBS-QB3 energy barriers, the global rate constant and the rate constant determined using analogy rules are reported in Fig. 6, while the cis and trans transition state structures for the minimum energy conformer are reported in Fig. S1 in the Supplemental Material. On the whole, given the approximations discussed above, we expect that the uncertainty factor for the rate constant calculated theoretically is within a factor of about 2–3. The ratio between the rate constant calculated using analogy rules and the one calculated theoretically using CBS-QB3 energy barriers is a factor of 1.3 in the 400–700 K temperature range (that is when the low temperature reactivity of CHPs is relevant) and grows to 2.0 using CCSD(T)/cc-pVTZ energy barriers corrected for basis set size effects with MP2/aug-cc-pVTZ energies. It can thus be concluded that the analogy rules allow calculating rate constants for H-abstraction reactions whose uncertainty is within the level that was considered reasonable to identify a major reaction channel in the present study.

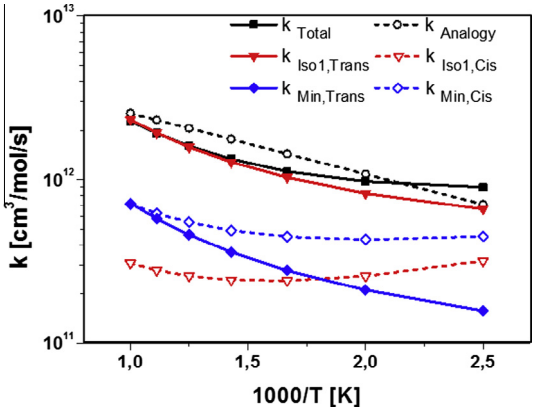

Fig. 6. Comparison between the rate constant calculated using analogy rules (K analogy) and the one determined theoretically (Ktot) summing up the rate constants of cis and trans addition to the minimum energy conformer of $CH_3COCH_2CH_2OOH$ (K minimum cis and K minimum trans) and those of the conformer that is closest in energy (K Iso1 cis and K Iso1 trans), weighted over the Boltzmann population of the conformers.

An analysis of which may be the product of the H-abstraction reaction was performed using an Intrinsic Reaction Coordinate (IRC) scan from the cis transition state of the minimum energy conformer. Simulations were performed starting from the transition state structure using a step of 0.1 Bohr updating the Hessian every 5 steps. It was found that following H-abstraction, an intermediate structure stabilized by the formation of a H bond with the O atom of the carbonyl group is formed, which successively loses the OH group and forms the molecule including two carbonyl groups, which was thus considered as the reaction product. Similarly, for the other H-abstraction reactions considered in this work, it was assumed that H-abstractions from carbonyl-hydroperoxides are followed by the fast decomposition of the radical product, as assumed in Fig. 2.

3.2. Carbonyl-hydroperoxide decomposition through the Korcek mechanism

The second set of reactions here investigated is the decomposition of CHPs through the Korcek mechanism. The mechanism of this reaction for 2-formyl-ethyl-hydroperoxide (C_3CHP) has been recently studied by Jalan et al. [38]. The reaction is started by a cyclization reaction to form a cyclic peroxide, which can subsequently decompose either to acetic acid and formaldehyde or to acetaldehyde and formic acid. The latter reaction channel is the fastest, while the rate determining step is the cyclization reaction. Beside H-abstraction reactions, cyclization is in competition with C_3CHP decomposition to OH radical, formaldehyde, and vinoxy radical. The rate constants of the cyclization reaction of C_3CHP and its analogous C_4CHP (2-acetyl-ethyl-hydroperoxide: $CH_3COCH_2CH_2OOH$ and 2-formyl-isopropyl-hydroperoxide: $CHOCH_2CHOOHCH_3$) were here computed using conventional transition state theory, correcting the rate constants for tunneling using the asymmetric Eckart model [44,45]. Channel specific rate constant for cyclic peroxide decomposition were computed using the rate parameters calculated by Jalan et al. [38] for the decomposition of the species formed by C_3CHP cyclization. The rate parameters calculated for the cyclization of C_3CHP and C_4CHP are reported in Table 1, while further details of the calculations are reported as Supplemental Material.

As it can be observed, the reaction of cyclization of $CHOCH_2CHOOHCH_3$ is about a factor of 5 faster than that calculated for C_3CHP,

Table 1
Rate parameters for the reaction of cyclization of C_3CHP and C_4CHP to the cyclic peroxide intermediate whose decomposition represent an important pathway for the formation of acids and aldehydes.

Temperature (K)	k_C (s^{-1})		
	C_3CHP	$CHOCH_2CHOOHCH_3$	$CH_3COCH_2CH_2OOH$
400[a]	4.2E−7	1.9E−6	1.9E−7
500[a]	3.6E−4	1.5E−3	1.8E−4
600[a]	3.6E−2	1.6E−1	2.1E−2
600[b]	1.5E−2	–	–
600[c]	1.3E−2	–	–

[a] Rate constants computed using CCSD(T)/CBS energy barriers.
[b] Rate constant calculated using the energy barrier computed at the CCSD(T)/cc-pVTZ level.
[c] Rate constant computed by Jalan et al. [38].

while the cyclization reaction of $CH_3COCH_2CH_2OOH$ is slightly slower. This is due to the different contribution of the additional methyl group for the two isomers, which hinders the rotational motion for $CHOCH_2CHOOHCH_3$ and favors that of $CH_3COCH_2CH_2$-OOH, thus leading to a decrease of the density of state for $CHOCH_2$-$CHOOHCH_3$ and to a slight increase for $CH_3COCH_2CH_2OOH$ with respect to C_3CHP. Channel specific rate constants were determined for the decomposition of the cyclic peroxide formed by $CHOCH_2$-$CHOOHCH_3$ using the same branching ratios used for C_3CHP. In the case of $CH_3COCH_2CH_2OOH$, the absence of the tertiary hydrogen in the cyclic peroxide intermediate implies that the only possible reac-tion channel is decomposition to acetic acid and acetaldehyde. The rate constants calculated for the fragmentation of C_3CHP and C_4CHP to the possible products and used in the simulations are sum-marized, with a schematic of Korcek mechanism in Fig. 7 (see also Table S1 of the Supplemental Material).

3.3. Molecular decomposition of acetyl-methyl-hydroperoxide

The last reaction that was studied is the concerted one step molecular decomposition of acetyl-methyl-hydroperoxide (CH_3-$COCH_2OOH$). The reason of this study is that, while H-abstraction reactions on CHP and the Korcek decomposition of CHP have the potential to explain the formation of several oxygenated species from propane and butane oxidation, the kinetic simulations reported in Fig. 11 clearly show that the predicted formation of acetic acid underestimates the experimental data. There is thus potential for the existence of alternative reaction routes. Here it is explored the molecular decomposition of acetyl-methyl-hydroperoxide, one of the simplest CHP species. Since this reaction has multireference character, as found calculating the T1 diagnostic of the CBS-QB3 transition state for decomposition to acetic acid, calculations were performed at the CASPT level. Computational details are reported as Supplemental Material. Though no transition state that directly connect the reactant to acetic acid could be found, two distinct three body transition states leading to decomposition into OH radical, formaldehyde, and the acetyl radical were found. A further transition state leading to the formation of a peroxide cyclic species similar to that of the Korcek mechanism was as well found. An internal reaction coordinate investigation of the two three body decomposition reactions showed that the product of both reactions are the acetyl radical and a complex formed by formaldehyde and the OH radical, stabilized by the formation of a hydrogen bond between the two. Barrier heights for the three reaction channels were determined on the geometries optimized using the minimal active space and the cc-pVDZ basis set increasing the basis set to the aug-cc-pVTZ level and the size of the active space. The calculated barrier heights are reported in Table 2.

The most interesting aspect of this system is that the final decom-position products of the reacting flux passing from the cis transition state may actually differ from the acetyl radical, OH, and formalde-hyde. An energy minimization performed starting from final step of the IRC scan of the cis transition state in fact converged to acetic acid and formaldehyde. An analysis of the intermediate geometries visited during the energy minimization protocol showed that fol-lowing dissociation from the hydroperoxy group the hydroxyl radi-cal remains in proximity of the acetyl radical center, so that after the $CH_3CO–CH_2OOH$ bond distance increases to about 3 Å it becomes possible to the hydroxyl group to react with CH_3CO and form acetic acid. This reaction path will be most probably in competition with the three body decomposition path, which will be progressively favored with increasing temperature, due to the higher density of states of its transition state, as it is the case for roaming reactions. However it is possible that at low temperatures, such as those con-sidered in the present work, a non-negligible contribution to the for-mation of minor reaction products may come from this pathway. Further studies are needed to determine whether this reaction mechanism may be competitive with the other low temperature reaction classes proposed in this work.

4. Comparisons with experimental measurements

All simulations required for the comparisons with the experimental measurements of the low temperature oxidation of propane and n-butane in JSR [8–14,33] were performed with OpenSMOKE code [46], with an extensive use of the BzzMath numerical library [47], by using the kinetic scheme POLIMI attached as Supplemental Material (in Chemkin format with thermo and transport properties), and also available in the Creck-Modeling web site (http://creckmodeling.chem.polimi.it).

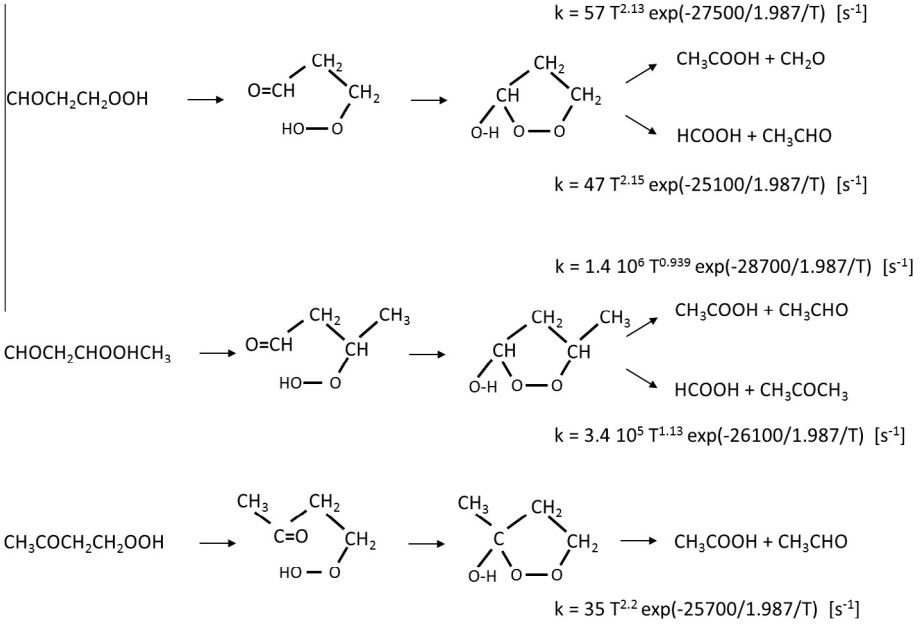

Fig. 7. Schematic of Korcek mechanism and rate constants for the decomposition of C_3CHP and C_4CHPs interpolated between 400 and 1000 K in the modified Arrhenius form.

Table 2
Barrier heights (kcal/mol) for the unimolecular decomposition of acetyl-methyl-hydroperoxide and for peroxy cyclization. Barrier heights are not corrected for Zero Point Energies, which were calculated from unscaled frequencies determined at the CASPT/cc-pVDZ level using the minimal active space here considered and are reported separately in the last column. All calculations performed at the CASPT2/aug-cc-pVTZ level using different active spaces.

Reaction	Energy barrier (kcal/mol)			ZPE correction
	(4e, 4o)	(6e, 6o)	(8e, 8o)	(4e, 4o)/(6e, 6o)
$CH_3COCH_2OOH \rightarrow CH_3CO + OH + H_2CO$ (cis)	44.6	45.7	44.7	−4.4
$CH_3COCH_2OOH \rightarrow CH_3CO + OH + H_2CO$ (trans)	44.8	46.6	45.7	−5.1
$CH_3COCH_2OOH \rightarrow$ C4 cyclization	–	46.2	45.8	−2.8

4.1. Low temperature oxidation of propane in JSR [11]

Cord et al. [11] investigated the low-temperature oxidation of propane using a jet-stirred reactor. Mole fractions of reactants and reaction products were measured as a function of the reactor temperature (550–730 K), with a particular attention to intermediate reaction products. As already mentioned, to widen the range of analyzed species, they used two different analytical methods: online gas chromatography (GC) in Nancy and synchrotron vacuum ultraviolet photoionization mass spectrometry (SVUV-PIMS) in Hefei. Experiments were performed under stoichiometric conditions with a large mole fraction of propane (0.12), at atmospheric pressure, residence time of 6 s, and the mixture was diluted in an inert gas (helium in Nancy and argon in Hefei). As shown in Fig. 1 and 1- and 2-propyl radicals additions on oxygen compete with their high temperature β-decomposition reactions to form ethylene and propene. Thus at low temperatures, two successive O_2 addition and isomerization reactions (occurring via intramolecular H-abstractions through cyclic transition states) form peroxy and propyl-hydroperoxy radicals up to the formation of three different carbonyl-hydroperoxides. Peroxy radicals can also form propyl hydroperoxides, mainly via recombination/disproportionation reactions with HO_2 radicals:

$$C_3H_7OO^{\cdot} + HO_2^{\cdot} \rightarrow C_3H_7OOH + O_2$$

All these hydroperoxides are the main source of the chain branching occurring at low temperatures. Detailed comparisons between experimental data and model predictions for propane, oxygen, and several intermediates are reported in Fig. 8. Simulations show that the system reactivity is not affected by the two different inert gases. This is firstly due to the very similar collisional efficiency of Ar and He adopted in POLIMI kinetic scheme. Moreover, it was also verified that the system sensitivity to collisional efficiency is very limited, at these low temperature conditions. The general agreement with major species is satisfactory. Hydro-gen peroxide and formaldehyde are under-predicted by a factor of 2–3, similar deviations were also observed by Cord et al. [11]. The detail of measured intermediate products was very useful to further validate the low temperature oxidation mechanism, and also to include in the kinetic scheme the new reaction paths of hydroperoxides, previously neglected. Particularly, the formation of several intermediate oxygenated species in the very low temperature region is well explained by adding to the previous mechanism H-abstraction and molecular reactions of hydroperoxides. As a matter of clarity, Fig. 8 also compares model predictions with and without these new reactions. The reduction of propane conver-sion is here less evident in comparison with n-butane results reported in Fig. 3. Nevertheless, the new reactions allow to improve the predictions of acetic acid and propyl-hydroperoxide and introduce new reaction channels to form oxirane, acetone, propanal, propanols, and C_3 components with two carbonyl groups, previously neglected.

Methyl-oxirane and oxetane are lumped into a single equivalent species (C_3-Cyclic ether), which is directly formed through the decomposition of C_3-hydroperoxy radicals (see Fig. 1) and well agrees with the experimental data. Similar agreement is also observed for methane, acetaldehyde, and propene, with an overestimation of ethylene in the NTC region. Methanol, properly predicted, is mostly obtained through the H-abstraction reactions of methoxy radicals on propane and different reaction products, such as formaldehyde and hydrogen peroxide. As already mentioned, an important source of acetic acid is the recombination reaction of peracetyl and methyl-peroxy radicals. The Korcek mechanism, i.e. the reaction pathways of carbonylhydroperoxide ($C_3H_6O_3$) forming the cyclic peroxide, which decomposes into acetic acid and formaldehyde [38]:

$$C_3H_6O_3 \rightarrow CH_2O + CH_3COOH$$

is included and it accounts for its remaining amount. The rate constant for this reaction channel was discussed in Section 3, and reported in Table S2 of the Supplemental Material.

The two C_3-hydroperoxides, lumped in the single equivalent component (C_3H_7OOH), are properly predicted with the complete model, while they are overestimated disregarding the H-abstraction reactions. As already shown in Fig. 4, the H-abstraction reactions on these hydroperoxides, with the successive fast decomposition of the intermediate radicals, are the effective paths to form acetone and propanal, at low temperatures. As far as the $C_3H_6O_3$ are concerned, 2-formyl-ethyl-hydroperoxide ($CHOCH_2$-CH_2OOH) is the prevailing one, due to the fast isomerization of the corresponding peroxy–hydroperoxy radical. It accounts for more than 90% of the lumped component $C_3H_6O_3$ considered in the POLIMI kinetic scheme. Thus, the following reactions, with the corresponding kinetic parameters of the H-abstraction by OH radicals, have been included in the mechanism:

$$^{\cdot}OH + C_3H_6O_3 \rightarrow H_2O + C_3\text{-dicarbonyls} + {}^{\cdot}OH$$
$$k = 3.5 \cdot 10^9 \exp(-630/RT)\ [m^3/kmol/s]$$

$$^{\cdot}OH + C_3H_6O_3 \rightarrow H_2O + \text{Acrolein} + HOO^{\cdot}$$
$$k = 1.75 \cdot 10^9 \exp(-630/RT)\ [m^3/kmol/s]$$

$$^{\cdot}OH + C_3H_6O_3 \rightarrow H_2O + CO + \text{Oxirane} + {}^{\cdot}OH$$
$$k = 5.9 \cdot 10^9 \exp(-630/RT)\ [m^3/kmol/s]$$

$$^{\cdot}OH + C_3H_6O_3 \rightarrow H_2O + CH_2CO + CH_2O + {}^{\cdot}OH$$
$$k = 4.8 \cdot 10^9 \exp(-630/RT)\ [m^3/kmol/s]$$

$$^{\cdot}OH + C_3H_6O_3 \rightarrow H_2O + CO + CH_3CHO + {}^{\cdot}OH$$
$$k = 1.2 \cdot 10^9 \exp(-630/RT)\ [m^3/kmol/s]$$

Kinetic parameters for the other H-abstracting radicals are obtained by applying the usual similarity and analogy rules [34]. Propandial ($CHOCH_2CHO$) is obtained via H-abstraction on 2-formyl-ethyl-hydroperoxide, while acetyl-methyl-hydroperoxide (CH_3COCH_2OOH) forms 2-oxopropanal (CH_3COCHO):

$$^{\cdot}OH + CHOCH_2CH_2OOH \rightarrow H_2O + CHOCH_2CHO + {}^{\cdot}OH$$

$$^{\cdot}OH + CH_3COCH_2OOH \rightarrow H_2O + CH_3COCHO + {}^{\cdot}OH$$

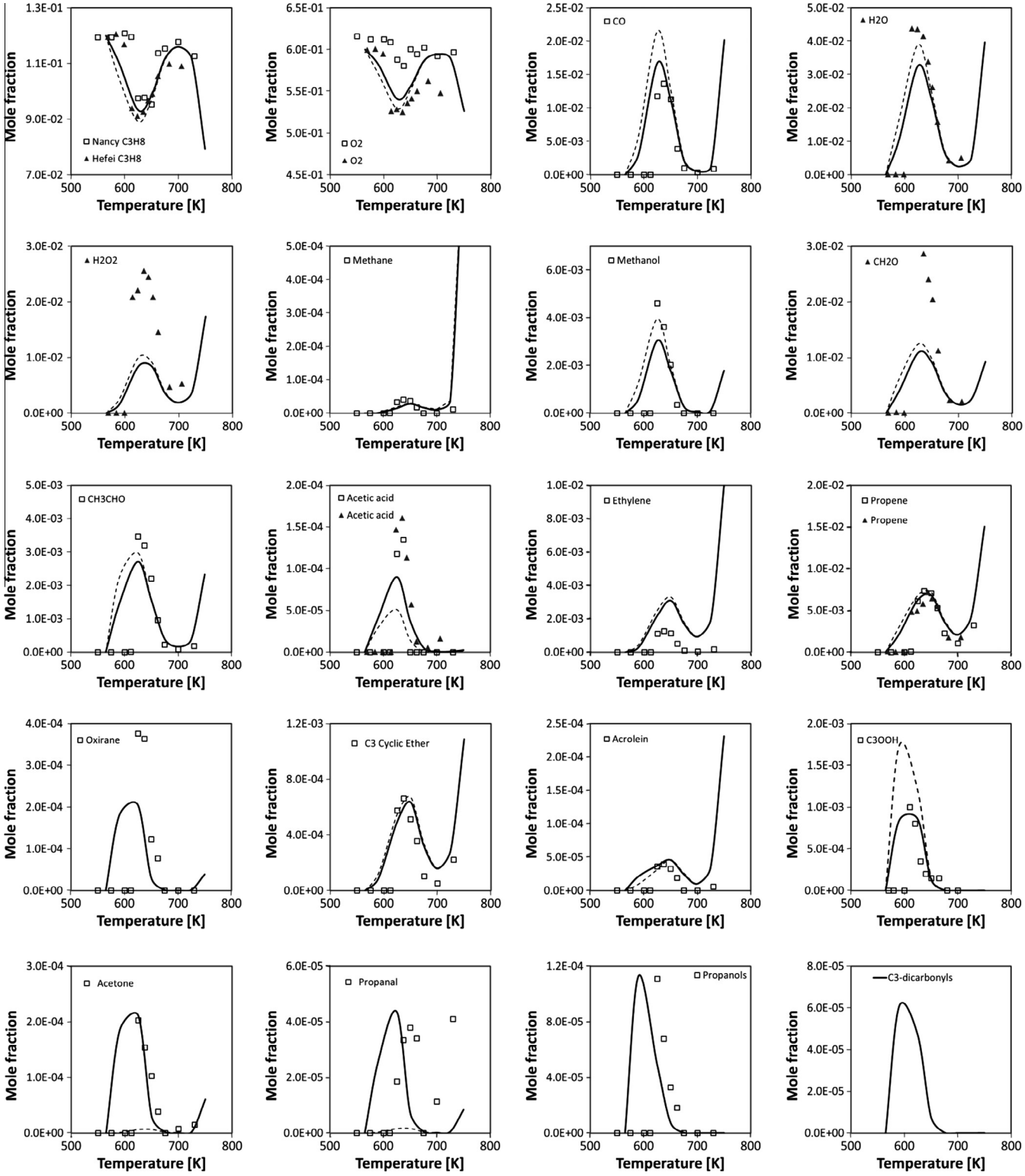

Fig. 8. Stoichiometric propane oxidation in a jet stirred reactor (12% C_3H_8; 1 atm; residence time 6 s) [11]. Mole fractions of major species and relevant intermediates at different reactor temperatures. Comparison of experimental measurements of Nancy [squares] and Hefei [triangles] with model predictions with [solid lines] and without [dashed lines] the new reactions.

both these C_3-dicarbonyl species are grouped into the lumped component ($C_3H_4O_2$).

The mole fraction profile of oxirane (C_2H_4O) shows a very sharp peak at the lowest temperatures, again suggesting its formation via H-abstraction reactions on $C_3H_6O_3$ and a fast decomposition of the intermediate radical ($\cdot COCH_2CH_2OOH$).

The formation of 1- and 2-propanol involves the recombination and disproportionation of propyl-peroxy radicals. While 1-propanol and propanal are obtained from the recombination of 1-propyl-peroxy radicals, 2-propanol and acetone are obtained from the recombination of two 2-propyl-peroxy radicals. Similarly, the formation of molecules with one hydroperoxy and one alcohol

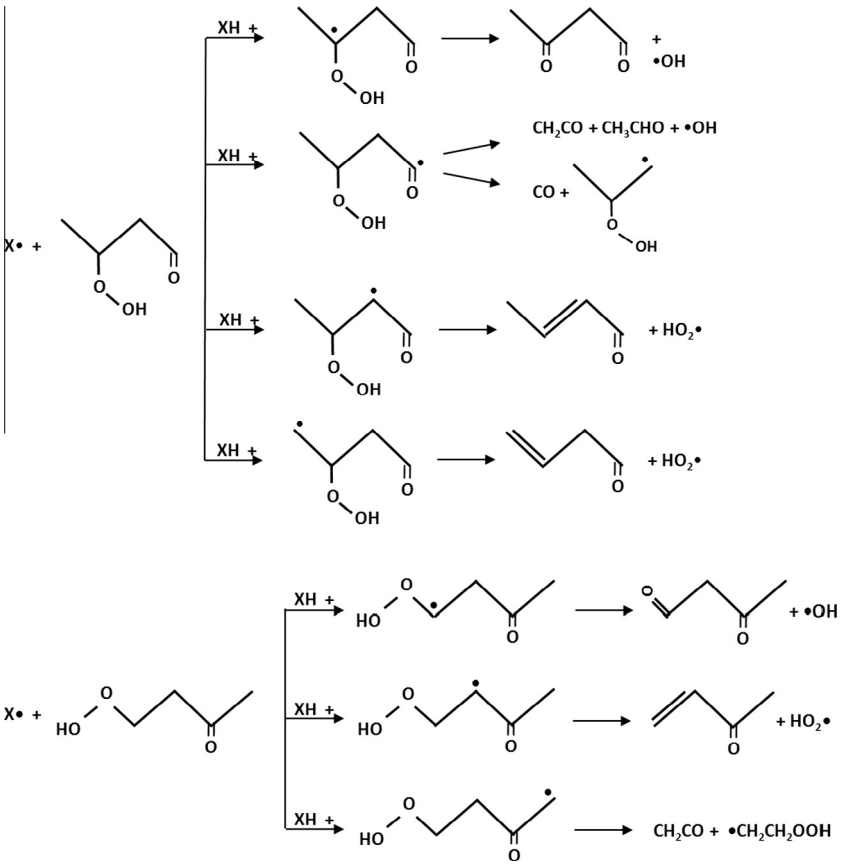

Fig. 9. H-abstraction reactions on the most favored C_4-carbonyl-hydroperoxides.

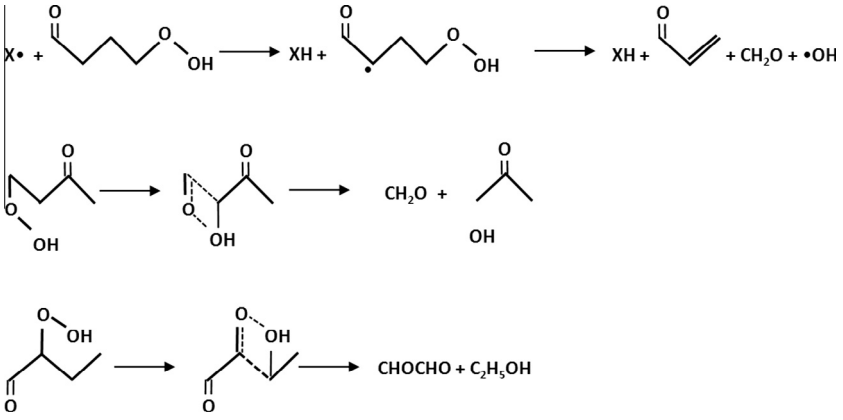

Fig. 10. Reaction paths to form acrolein, acetol, glyoxal, ethanol, and acetic acid.

functions can be explained with the recombination and disproportionation reactions of peroxy–hydroperoxy radicals.

Finally, Fig. 8 also shows the expected mole fractions of C_3-molecules including two carbonyl groups ($C_3H_4O_2$) not measured by Cord et al. [11]. In similar low temperature experiments, Herbinet et al. [10] mentioned relative errors of carbon balances up to 20%, mainly due to the non-quantification of some oxygenated species in the very low temperature conditions.

4.2. n-Butane in Nancy and Hefei stirred reactor [9,12]

As already partially shown in Fig. 3, the low-temperature oxidation of n-butane in a jet-stirred reactor was presented and discussed by Herbinet et al. [9] and Cord et al. [12]. Experiments were performed at 1.06 [9] and 1.0 [12] atm, for temperatures between 550 and 800 K, at a mean residence time of 6 s and with a stoichiometric n-butane/oxygen/argon mixture (4/26/70 in mol%). Similar experiments with a stoichiometric n-butane/O_2/helium mixture (2.3/15/82.7 in mol%) were also presented by Bahrini et al. [13,14]. A detailed kinetic model [8] was able to reproduce the global reactivity and the major oxidation products, while the predictions of alcohols, ketones, diones, and acetic acid were not completely satisfactory [12,33].

While the formation of organic acids can be explained with the Korcek mechanism [38], the H-abstraction reactions on the most favored C_4-carbonyl-hydroperoxides reported in Fig. 9 show simple channels to form not only C_4-dicarbonyl species, but also ketene, acetaldehyde, methyl-vinyl-ketone, and 1- and 2-butenal.

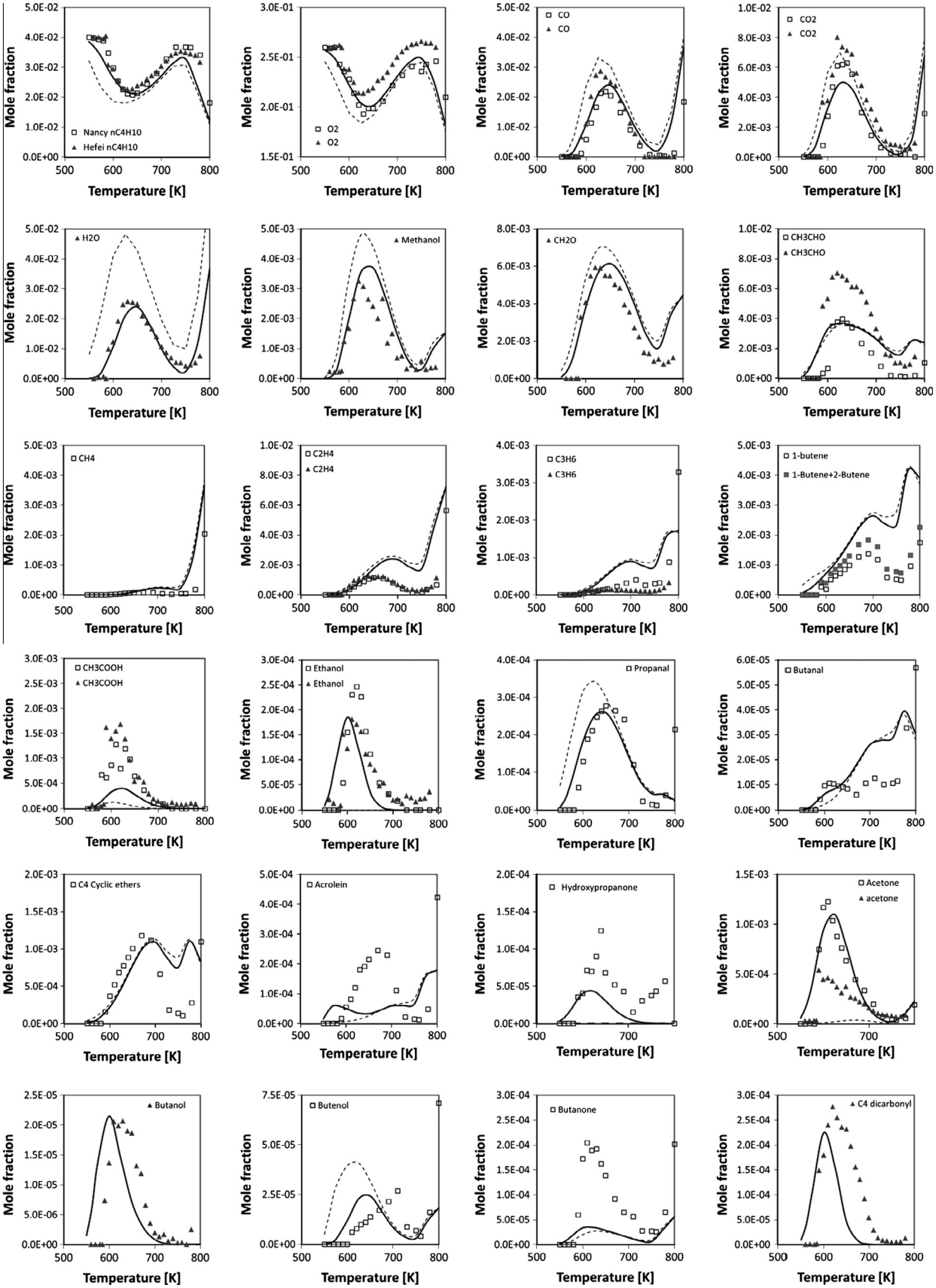

Fig. 11. Oxidation of n-butane in jet stirred reactor (n-butane/O_2/Ar = 4/26/70 mol%; 1 atm; residence time 6 s) [9,12]. Mole fractions of relevant intermediates at different reactor temperatures. Comparison of experimental measurements of Nancy [squares] and Hefei [triangles] with model predictions with [solid lines] and without [dashed lines] the new reactions. Note that butanol predictions are compared with the signal of mass 74 amu profile [48].

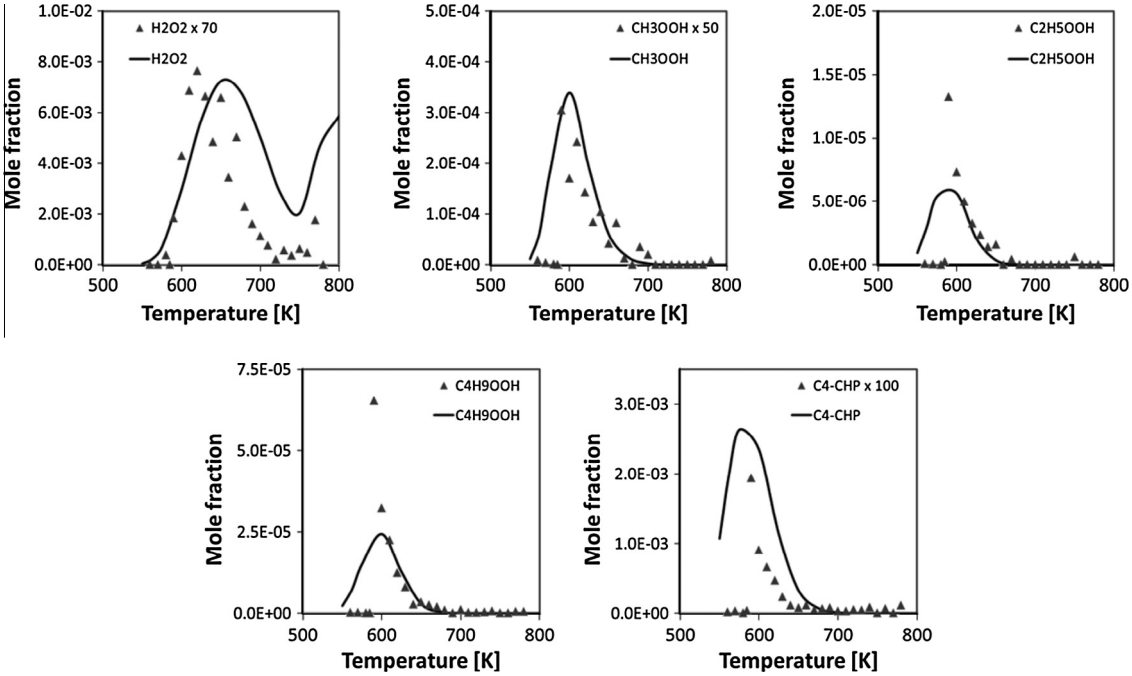

Fig. 12. Oxidation of n-butane in jet stirred reactor (n-butane/O_2/Ar = 4/26/70 mol%; 1 atm; residence time 6 s) [9,12]. Mole fractions of hydrogen peroxide, alkyl-hydroperoxides, and carbonyl-hydroperoxides at different reactor temperatures. Comparison of experimental measurements of Hefei [triangles] with model predictions [lines].

Figure 11 reports detailed comparisons between experimental data [9,12,48] and predictions of POLIMI kinetic scheme, with and without the new reactions.

The reactivity of the system, oxygen consumption, and the NTC region are well reproduced by the model together with major oxidation products. As far as the differences in acetaldehyde measurements of Nancy and Hefei are concerned, the model better agrees with Nancy measurements. Model over-predictions of ethylene, propene and butenes are present, mainly at 700–800 K in the NTC zone, and they are mainly due to the decomposition of the alkyl-hydroperoxy radicals. This decomposition is also responsible of the over-prediction of cyclic ethers with 4 carbon atoms (methyl-oxetane, dimethyl-oxirane, ethyl-oxirane, and tetrahy-dro-furan) grouped in a single lumped component. As already mentioned, the differences between the two model predictions are limited to the temperature range 550–650 K. More than the dif-ferent reactivity, it is important to underline that the new reactions allow to predict several species that were previously completely neglected (butanol, hydroxypropanone, and C4-dicarbonyl com-pounds) and also to improve the predictions of other components strongly underestimated (acetic acid, ethanol, and acetone). The experimental mole fraction of several species show a very sharp onset when reaction starts, whereas the model shows a smoother behavior. While the wall reactions are proved to have influence mainly at higher temperatures [9], we suspect that these deviations, in the order of 20–30 K, could be partially due to wall effects.

Measured mole fraction of acetic acid overcomes 1000 ppm and it is more than three times the amount observed in propane oxidation, despite the higher dilution. The previous radical path, via peracetyl radicals gives here only a contribution of ~30%, while the Korcek reaction route plays a major role. The decomposition products of the two C_4-ketohydroperoxide isomers through the Korcek mechanism can be either acetic acid and acetaldehyde [38] or acetone and formic acid, through the formic conformer of the cyclic peroxide. Details on rate parameters and mechanistic aspects were discussed in Section 3 and are reported in Table S2 of the Supplemental Material.

Butanone or methyl-ethyl-ketone (MEK) is largely under-predicted. It is mainly formed via the recombination/disproportionation of peroxy–hydroperoxy and methylperoxy radicals, while the contribution of the H-abstraction reactions on C_4-hydroperoxide is in the order of 10%.

Further possible reactions to explain the significant formation of ethanol, acetol and acrolein are shown in Fig. 10. While acrolein and formaldehyde can be obtained through the fast decomposition of an intermediate radical of H-abstraction reactions on 1-formyl-3-propyl-hydroperoxide, acetol (hydroxypropanone) and formaldehyde are the possible products of a four center reaction of 2-acetyl-ethyl-hydroperoxide. Finally, another four center molecular reaction of 1-formyl-1-propyl-hydroperoxide can explain ethanol formation. The feasibility of the molecular reaction pathways reported in Fig. 10 was discussed in Section 3, while the rate constants of the H-abstraction reactions are estimated through the similarity rules [34] and are not further theoretically investigated.

Figure 12 shows a comparison between model predictions and experimental measurements of hydroperoxide species. While the comparisons are reasonable for C_2- and C_4-hydroperoxides, large differences are observed for H_2O_2, CH_3OOH, and C_4CHP. For this reason, scaling factors are applied to the experimental data of Fig. 12. Large deviations were also observed by Herbinet et al.[9], and there are critical uncertainties on these difficult experi-mental measurements [48]. It is indeed surprising to have this large over-prediction of H_2O_2, while there was an under-prediction in Fig. 8 for propane oxidation.

Bahrini et al. [13,14] have quantified H_2O_2 during n-butane oxidation in a jet-stirred reactor under conditions very close to those used by Herbinet et al. [9] using continuous wave cavity ring-down spectroscopy (cw-CRDS) in the near-infrared. This analytical system is expected to give accurate measurements of hydroperoxides, and relative uncertainties for different species are also discussed [13,14]. Moreover, accepting a scarce influence of the inert gas, the two independent sets of experimental data on propane and n-butane give further indication of experimental uncertainties in these measurements. Figure 13 shows a few comparisons between

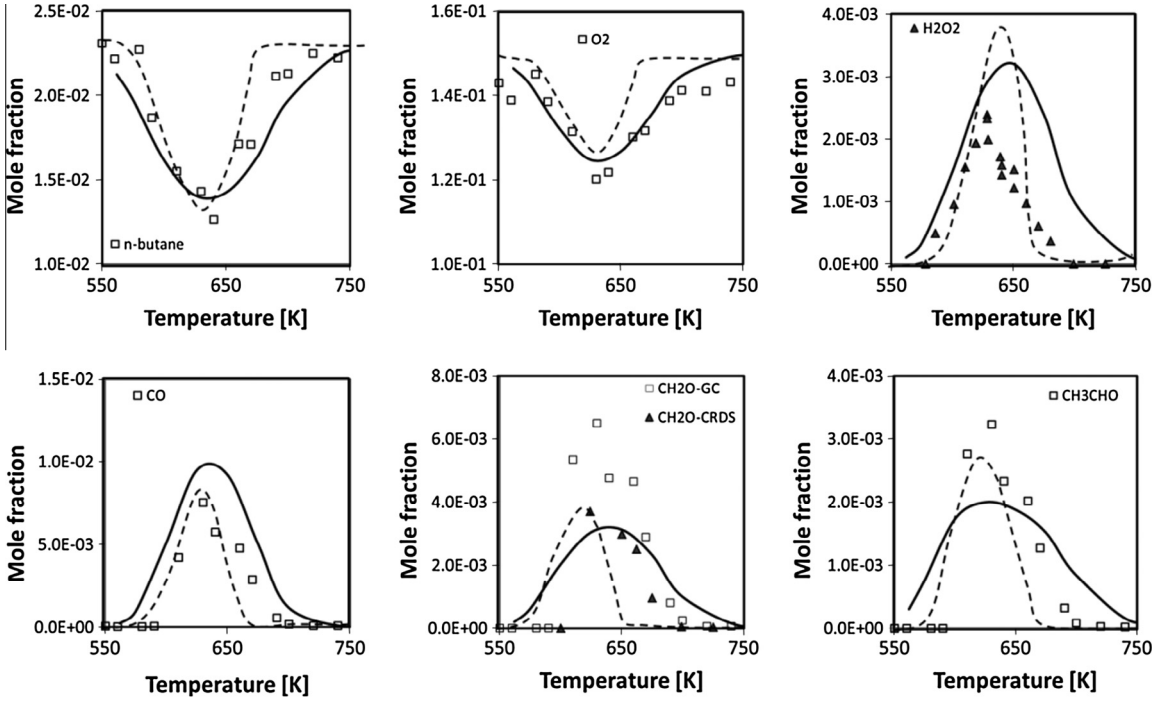

Fig. 13. Oxidation of n-butane in jet stirred reactor (n-butane/O_2/He = 2.3/15/82.7 mol%; p = 1 atm; residence time 6 s) [13,14]. Mole fractions of n-butane, oxygen and relevant products. Comparison between experimental data [GC: squares and CRDS: triangles] and predictions of POLIMI [solid lines] and Nancy [dashed lines] kinetic schemes.

experimental measurements [13,14] and predictions obtained with both the POLIMI and the Nancy kinetic schemes [13,14]. Both the models give satisfactory agreement with these major species, including H_2O_2. The NTC region predicted by POLIMI is slightly wider with respect to the experimental data, while the reverse is observed with the Nancy model. Nevertheless, the better agreement with H_2O_2 mole fractions supports the uncertainty of the previous H_2O_2 measurements (Fig. 12). A more complete comparison between these experimental measurements [13,14] and the predictions of POLIMI kinetic scheme is reported in the Supplemental Material of this paper.

5. Conclusions

After twenty years since the first kinetic mechanism of propane and butane oxidation [26], the careful kinetic analysis of recent detailed data allows to highlight the importance of three new reaction classes, previously neglected in the low temperature mechanisms. Particularly, the following reaction classes are likely to be added to these mechanisms:

1. H-abstraction reactions on hydroperoxides and carbonyl-hydroperoxides, to form carbonyl and dicarbonyl components.
2. Molecular reactions of carbonyl-hydroperoxides (Korcek mechanism [38]), to form organic acids.
3. Recombination/disproportionation reactions of peroxy radicals, to form alcohols, ketones and species containing two oxygenated groups.

It is important to underline that these reactions are effective only at very low temperatures (550–650 K), reducing the overall reactivity of the system, and mainly explaining the important formation of organic acids and minor oxygenated species. The extension of the overall kinetic mechanism, with the addition of these new reaction classes for heavier hydrocarbon fuels, already allows satisfactory comparisons also with the reaction products of the low temperature oxidation of n-heptane [10,49]. Finally, preliminary theoretical calculations already show the reliability of these reaction paths in justifying the formation of these species and point out the need of further research activities in the investigation of successive reactions of hydroperoxide species. Similar conclusions on this topic were also very recently drawn by Herbinet and Battin Leclerc [33].

Acknowledgments

Authors gratefully acknowledge Dr. Frédérique Battin-Leclerc and Dr. Olivier Herbinet for providing the experimental data of Figs. 3, 8 and 11–13.

Appendix A. Supplementary material

Supplementary data associated with this article can be found, in the online version.

References

[1] J. Zádor, C.A. Taatjes, R.X. Fernandes, Prog. Energy Combust. Sci. 37 (4) (2011) 371–421.
[2] R.T. Pollard, in: C.H. Bamford, C.F.H. Tipper (Eds.), Comprehensive Chemical Kinetics: Gas Phase Combustion, vol. 17, Elsevier, New York, 1977, pp. 249–367.
[3] M.J. Pilling, Low Temperature Combustion and Autoignition, Elsevier, Amsterdam, The Netherlands, 1997.
[4] C.K. Westbrook, Proc. Combust. Inst. 28 (2) (2000) 1563–1577.
[5] J.M. Simmie, Prog. Energy Combust. Sci. 29 (6) (2003) 599–634.
[6] F. Battin-Leclerc, Prog. Energy Combust. Sci. 34 (4) (2008) 440–498.
[7] C.F. Goldsmith, W.H. Green, S.J. Klippenstein, J. Phys. Chem. A 116 (13) (2012) 3325–3346.
[8] F. Battin-Leclerc, O. Herbinet, P.-A. Glaude, R. Fournet, Z. Zhou, L. Deng, H. Guo, M. Xie, F. Qi, Proc. Combust. Inst. 33 (1) (2011) 325–331.
[9] O. Herbinet, F. Battin-Leclerc, S. Bax, H. Le Gall, P.-A. Glaude, R. Fournet, Z. Zhou, L. Deng, H. Guo, M. Xie, Phys. Chem. Chem. Phys. 13 (1) (2011) 296–308.

[10] O. Herbinet, B. Husson, Z. Serinyel, M. Cord, V. Warth, R. Fournet, P.A. Glaude, B. Sirjean, F. Battin-Leclerc, Z. Wang, Combust. Flame 159 (12) (2012) 3455–3471.
[11] M. Cord, B. Husson, J.C. Lizardo Huerta, O. Herbinet, P.A. Glaude, R. Fournet, B. Sirjean, F. Battin-Leclerc, M. Ruiz-Lopez, Z. Wang, J. Phys. Chem. A 116 (50) (2012) 12214–12228.
[12] M. Cord, B. Sirjean, R. Fournet, A. Tomlin, M. Ruiz-Lopez, F. Battin-Leclerc, J. Phys. Chem. A 116 (24) (2012) 6142–6158.
[13] C. Bahrini, O. Herbinet, P.-A. Glaude, C. Schoemaecker, C. Fittschen, F. Battin-Leclerc, J. Am. Chem. Soc. 134 (29) (2012) 11944–11947.
[14] C. Bahrini, P. Morajkar, C. Schoemaecker, O. Frottier, O. Herbinet, P.-A. Glaude, F. Battin-Leclerc, C. Fittschen, Phys. Chem. Chem. Phys. 15 (45) (2013) 19686–19698.
[15] P. Dagaut, M. Reuillon, M. Cathonnet, Combust. Flame 101 (1) (1995) 132–140.
[16] R. Minetti, M. Carlier, M. Ribaucour, E. Therssen, L. Sochet, Combust. Flame 102 (3) (1995) 298–309.
[17] P. Gaffuri, T. Faravelli, E. Ranzi, N.P. Cernansky, D. Miller, A. d'Anna, A. Ciajolo, AIChE J. 43 (5) (1997) 1278–1286.
[18] H. Curran, P. Gaffuri, W.J. Pitz, C.K. Westbrook, Combust. Flame 114 (1–2) (1998) 149–177.
[19] E. Ranzi, A. Frassoldati, S. Granata, T. Faravelli, Ind. Eng. Chem. Res. 44 (14) (2005) 5170–5183.
[20] J. Biet, M.H. Hakka, V. Warth, P.-A. Glaude, F. Battin-Leclerc, Energy Fuels 22 (4) (2008) 2258–2269.
[21] C. Westbrook, W. Pitz, M. Mehl, H. Curran, Proc. Combust. Inst. 33 (1) (2011) 185–192.
[22] S. Sarathy, C. Westbrook, M. Mehl, W. Pitz, C. Togbe, P. Dagaut, H. Wang, M. Oehlschlaeger, U. Niemann, K. Seshadri, Combust. Flame 158 (12) (2011) 2338–2357.
[23] C.K. Westbrook, J. Warnatz, W.J. Pitz, A detailed chemical kinetic reaction mechanism for the oxidation of iso-octane and n-heptane over an extended temperature range and its application to analysis of engine knock, in: Symposium (International) on Combustion, 1989, Elsevier, 1989, pp. 893–901.
[24] E. Ranzi, T. Faravelli, P. Gaffuri, A. Sogaro, Combust. Flame 102 (1) (1995) 179–192.
[25] F. Buda, R. Bounaceur, V. Warth, P.-A. Glaude, R. Fournet, F. Battin-Leclerc, Combust. Flame 142 (1) (2005) 170–186.
[26] E. Ranzi, T. Faravelli, P. Gaffuri, G. Pennatti, A. Sogaro, Combust. Sci. Technol. 100 (1–6) (1994) 299–330.
[27] H.J. Curran, P. Gaffuri, W. Pitz, C. Westbrook, Combust. Flame 129 (3) (2002) 253–280.
[28] R. Fournet, F. Battin-Leclerc, P. Glaude, B. Judenherc, V. Warth, G. Come, G. Scacchi, A. Ristori, G. Pengloan, P. Dagaut, Int. J. Chem. Kinet. 33 (10) (2001) 574–586.
[29] E. Ranzi, T. Faravelli, P. Gaffuri, E. Garavaglia, A. Goldaniga, Ind. Eng. Chem. Res. 36 (8) (1997) 3336–3344.
[30] C.K. Westbrook, W.J. Pitz, O. Herbinet, H.J. Curran, E.J. Silke, Combust. Flame 156 (1) (2009) 181–199.
[31] E. Ranzi, A. Frassoldati, T. Faravelli, A. Cuoci, Energy Fuels 23 (10) (2009) 5287–5289.
[32] F. Battin-Leclerc, A. Konnov, J.-L. Jaffrezo, M. Legrand, Combust. Sci. Technol. 180 (2) (2007) 343–370.
[33] O. Herbinet, F. Battin-Leclerc, Int. J. Chem. Kinet. 46 (10) (2014) 619–639.
[34] E. Ranzi, M. Dente, T. Faravelli, G. Pennati, Combust. Sci. Technol. 95 (1–6) (1993) 1–50.
[35] R. Atkinson, D. Baulch, R. Cox, J. Crowley, R. Hampson, R. Hynes, M. Jenkin, M. Rossi, J. Troe, I. Subcommittee, Atmos. Chem. Phys. 6 (11) (2006) 3625–4055.
[36] A.S. Hasson, G.S. Tyndall, J.J. Orlando, J. Phys. Chem. A 108 (28) (2004) 5979–5989.
[37] J.J. Orlando, G.S. Tyndall, T.J. Wallington, Chem. Rev. 103 (12) (2003) 4657–4690.
[38] A. Jalan, I.M. Alecu, R.n. Meana-Pañeda, J. Aguilera-Iparraguirre, K.R. Yang, S.S. Merchant, D.G. Truhlar, W.H. Green, J. Am. Chem. Soc. 135 (30) (2013) 11100–11114.
[39] E. Ranzi, A. Sogaro, P. Gaffuri, G. Pennati, T. Faravelli, Combust. Sci. Technol. 96 (4–6) (1994) 279–325.
[40] J.M. Martin, Chem. Phys. Lett. 259 (5) (1996) 669–678.
[41] D.E. Woon, T.H. Dunning Jr., J. Chem. Phys. 103 (11) (1995) 4572–4585.
[42] Gaussian 09, Revision C.01, M.J. Frisch, G.W. Trucks, H.B. Schlegel, G.E. Scuseria, M.A. Robb, J.R. Cheeseman, G. Scalmani, V. Barone, B. Mennucci, G.A. Petersson, H. Nakatsuji, M. Caricato, X. Li, H.P. Hratchian, A.F. Izmaylov, J. Bloino, G. Zheng, J.L. Sonnenberg, M. Hada, M. Ehara, K. Toyota, R. Fukuda, J. Hasegawa, M. Ishida, T. Nakajima, Y. Honda, O. Kitao, H. Nakai, T. Vreven, J.A. Montgomery, Jr., J.E. Peralta, F. Ogliaro, M. Bearpark, J.J. Heyd, E. Brothers, K.N. Kudin, V.N. Staroverov, R. Kobayashi, J. Normand, K. Raghavachari, A. Rendell, J.C. Burant, S.S. Iyengar, J. Tomasi, M. Cossi, N. Rega, J.M. Millam, M. Klene, J.E. Knox, J.B. Cross, V. Bakken, C. Adamo, J. Jaramillo, R. Gomperts, R.E. Stratmann, O. Yazyev, A.J. Austin, R. Cammi, C. Pomelli, J.W. Ochterski, R.L. Martin, K. Morokuma, V.G. Zakrzewski, G.A. Voth, P. Salvador, J.J. Dannenberg, S. Dapprich, A.D. Daniels, Farkas, J.B. Foresman, J.V. Ortiz, J. Cioslowski, D.J. Fox, Gaussian, Inc., Wallingford CT, 2009.
[43] H. Werner, P. Knowles, R. Lindh, F. Manby, M. Schütz, in: MOLPRO, version, 2008.
[44] C. Eckart, Phys. Rev. 35 (11) (1930) 1303.
[45] C. Cavallotti, D. Polino, A. Frassoldati, E. Ranzi, J. Phys. Chem. A 116 (13) (2012) 3313–3324.
[46] A. Cuoci, A. Frassoldati, T. Faravelli, E. Ranzi, Open SMOKE: numerical modeling of reacting systems with detailed kinetic mechanisms, in: XXXIV Meeting of the Italian Section of the Combustion Institute, 2011, 2011.
[47] G. Buzzi-Ferraris, F. Manenti, Comput. Aided Chem. Eng. 30 (2) (2012) 1312–1316.
[48] F. Battin-Leclerc, O. Herbinet, Personal Communication (2014).
[49] M. Pelucchi, M. Bissoli, C. Cavallotti, A. Cuoci, T. Faravelli, A. Frassoldati, E. Ranzi, A. Stagni, Energy Fuels 28 (11) (2014) 7178–7193.